Journal of Oceanology and Limnology
Vol. 36 No. 1, P. 165-180, 2018
https://doi.org/10.1007/s00343-018-7136-3

Ferroan dolomites in Miocene sediments of the Xisha Islands and their genetic model*

XU Hong (许红)[1, 2, **], ZHANG Weiwei (张威威)[1, 3], WEI Kai (魏凯)[1, 3], HE Qingkun (赫庆坤)[4], JIANG Yunshui (江云水)[1, 2], XU Tingting (许婷婷)[1, 2], JIANG Xuejun (姜学钧)[1, 2], YAN Guijing (闫桂京)[1, 2], SONG Hongying (宋红瑛)[4], WANG Jianghai (王江海)[5, **]

[1] *Key Laboratory of Marine Hydrocarbon Resources and Environment Geology*, *Qingdao Institute of Marine Geology*, *Ministry of Land and Resources*, *Qingdao 266071*, *China*

[2] *Laboratory for Marine Mineral Resources*, *Qingdao National Laboratory for Marine Science and Technology*, *Qingdao 266071*, *China*

[3] *China University of Petroleum* (*East China*), *Qingdao 266555*, *China*

[4] *Shandong University of Science and Technology*, *Qingdao 266590*, *China*

[5] *Guangdong Provincial Key Laboratory of Marine Resources and Coastal Engineering/South China Sea Bioresource Exploitation and Utilization Collaborative Innovation Center*, *School of Marine Sciences*, *Sun Yat-Sen University*, *Guangzhou 510006*, *China*

Received May 3, 2017; accepted in principle Jun. 21, 2017; accepted for publication Aug. 28, 2017

Abstract Carbonate rocks are important reservoirs for global petroleum exploration. The largest oilfield in the South China Sea, Liuhua 11-1, is distributed in the massive carbonate reef area of the Zhujiang (Pearl) River Mouth Basin. Previous studies showed that one 802.17-m-long core from well Xichen-1 in the South China Sea mainly consisted of white and light gray-white organic reefs. Recently, a Miocene whole core (161.9 m long) of well Xiyong-2, near well Xichen-1, was found to contain six layers of yellowish brown, light yellowish gray, iron black, or light yellowish gray-white organic reefs. Scanning electron microscope images of these layers reveal a typical ferroan dolomite rich in Fe (up to 29%), with the high concentrations of Mn, Cu, W, Zn, Cr, Ni, and Co. Systematic X-ray powder diffraction analysis yields a 1.9–6.1 match in phase ratio with ankerite, 5.4–26.9 with dolomite, and zero with calcite, which indicate that the samples can be classified as ferroan dolomite. The iron and heavy metals are inferred to be originated from multiple volcanic eruptions of Gaojianshi Island in the Dongdao Atoll during the middle-late Miocene. These elements were dissolved in seawater, likely as a sol, and carried to Yongxing Island in the Xuande Atoll by sea currents and tides enhanced by prevailing winds, and deposited as a part of the sedimentation process in the study area. The ferroan dolomite has Sr content of $(125–285)\times10^{-6}$, which is lower than the accepted Sr boundary value of dolomite. This finding suggests that dolomitization occurred during large-scale global glacial regression in the late Miocene. The isolated Xisha carbonate platform, exposed to air, underwent freshwater leaching and dolomitization induced by mixed water, and caused the extensive Fe-Mg exchange along the organic reef profile to form ankerite and ferroan dolomite. These results may help to understand paleoceanographic environmental changes in the South China Sea during the Miocene.

Keyword: ferroan dolomite; X-ray powder diffraction; sedimentation mechanism; Miocene; Xisha Islands

1 INTRODUCTION

The Xisha Islands, part of an isolated carbonate platform in the northwestern part of the South China Sea, include organic reef islands. Within the island group, Gaojianshi Island is the only one that originated from volcanic eruptions. It reaches 7 m above the sea level in elevation and 15 m in width, has an area of 0.04 km^2, and lies about seven nautical miles

* Supported by the National Basic Research Program of China (973 Program) (No. 2012CB956004), the Science and Technology Basic Resources Investigation Program of China (No. 2017FY201407), the National Oil and Gas Major Projects of China (No. 2011ZX05025-002), and the National Natural Science Foundation of China (NSFC) (No. 41106064)
** Corresponding authors: qdxhong@163.com; wangjhai@mail.sysu.edu.cn

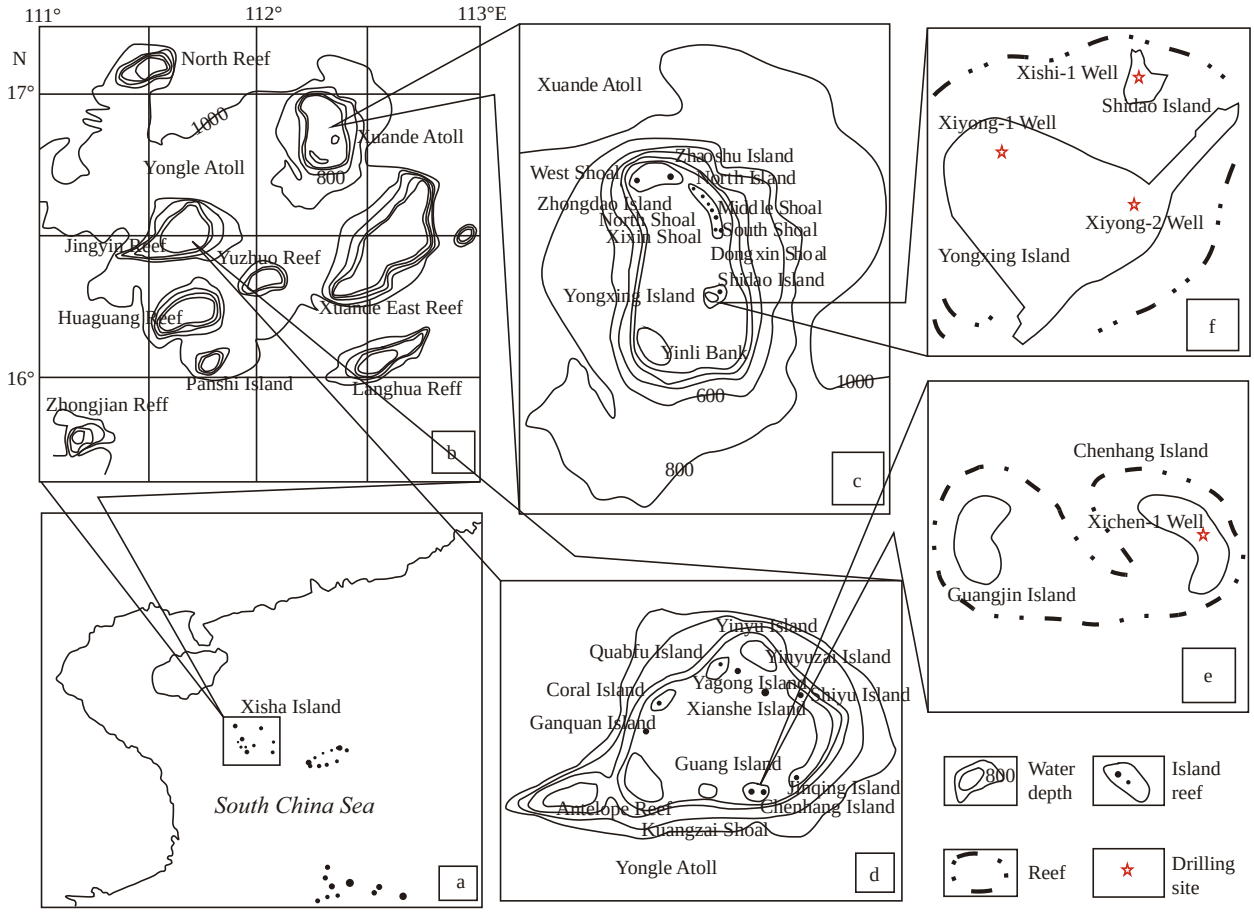

Fig.1 Maps showing the atolls and locations of wells Xichen-1, Xiyong-1, and Xiyong-2 on the Xisha Islands

southwest of the Dongdao Atoll. It is composed of volcanic breccia of limburgite with a K-Ar age of 2.05 Ma, and has been used to study neotectonic movements (Zhan et al., 2006).

Research on the Xisha organic reefs began nearly four decades ago, and geological field observations have been performed at four field sites (Fig.1). Drilling of the well Xiyong-1 was completed in 1979, reached a depth of 1 384.68 m, and penetrated a bioherm at a depth of 1 251 m. Previously, only two of the other three whole-core wells had reached Miocene strata (Xu et al., 1999a). The cores from these two wells were previously used to study the bioherm characteristics, formation rocks, sedimentation, post-diagenetic biologic evolution (especially the mechanism of dolomitization), paleoceanographic changes, and reservoir properties of the bioherm (Ye et al., 1984, 1985a; He and Zhang, 1986; Lü et al., 1986, 1987; Wang et al., 1986; Zhang et al., 1987, 1989; He and Zhang, 1990; Xu et al., 1994, 1999a; Wei et al., 2006, 2007, 2008). The dark reefal sediments were interpreted to be of volcanic origin. Yan et al. (2002) found a 3.1-m-thick black layer at a depth of less than 100 m in well Nanyong-2. In this study, the dark volcanic sediments were found to be thicker than 100 m and of Miocene age.

Studies of the shallow reefal sections from well Xiyong-2 began in 1985. Zhang et al. (1989) regarded the unconformity at the depth of 256 m as the bottom boundary of the Pleistocene based on lithological characteristics, and reported that below this depth was a 1.42-m-thick hard layer of dolomized algal wackestone, which would indicate the prolonged subaerial exposure. However, Meng (1989) analyzed planktonic foraminiferal assemblages and concluded that the base of the Pleistocene was at a depth of 235 m. In light of the consistency of planktonic foraminiferal assemblages across the Tertiary-Quaternary boundary, we consider Meng's proposed placement of the lower boundary of the Pleistocene to be more reliable; the unconformity at 256 m depth may be related to frequent sea-level changes in the Pliocene.

Meng (1989) fixed the bottom boundary of the

Pliocene at the depth of 235 m, but a set of lagoonal wackestone occurred at this depth, and there was no clear petrological evidence of a single consistent stratigraphic boundary. Moreover, C, Ca, Mg and Sr contents, as well as oxygen isotope ratios, were continuous at this depth. Therefore, Zhang et al. (1989) moved the lower boundary of the Pliocene down to a core depth of 377 m. Dolomite was found below this depth in well Xiyong-2, which coincided with a large unit of dolomite below the depth of 370 m in well Xiyong-1. These two wells are 1 km apart, and their dolomite layers appear to share the same origin. These findings correlate well with the Miocene dolomite of well Xichen-1. Therefore, the unconformity at the depth of 377 m has been interpreted as the bottom boundary of the Pliocene in well Xiyong-2 (Meng, 1989; Han and Meng, 1990).

Based on the above division, the interval from the core depth of 390.04 m to the well bottom at 600.33 m (a total of 210.29 m) in well Xiyong-2 can be dated as Miocene in age. This interval was cored from 76 round trips. The core was sealed in storage until July 2011 when the first logging investigation was conducted. Below the depth of 391.9 m, various layers of loose and hard sediments were observed. The specimens were iron brown. The bioherm layer was approximately 51 cm in thickness, and intercalated with several thin gray to white limestone interlayers (Fig.2).

In this work, we present new data from dolomites, which are important not only for indicating the presence of ferroan dolomite and associated sedimentary facies, as well as its genetic model, but also for providing a novel clue to trace the Neogene volcanic activity, glaciation events, and paleoceanographic and environmental changes in the South China Sea.

2 MATERIAL AND METHOD

Systematic and specific core logging at different depths below 390.04 m in well Xiyong-2 included descriptive analysis, imaging, partial X-ray 3D scanning, and sampling at intervals of 0.2–0.35 m. The logging data were used to correlate petrological sections of the same well or different wells in the same drilling area.

Thin sections were cut from the core, analyzed under a polarizing microscope, and correlated with typical volcanic pumices from Dongdao Island. Sample No. 9 was collected at the depth of 494.3–494.7 m in well Xiyong-2, and was composed of dolomites with iron-bearing clastic sediments. Sample No. 9 was used for an example analysis, and 16 additional samples were then collected along the core profile for further analyses, including for mineralogy, lithology, petrology and multiple electronic microanalysis. Details of the analytical methods are presented below.

Twenty-eight conventional (28 mm×49 mm) and super-large (49 mm×75 mm) thin sections were prepared at the China University of Petroleum (East China). The mineralogical, petrological and biological features of these samples were successively examined via optical microscopy, scanning electron microscopy (SEM), electron probe, X-ray powder diffraction (XRD), inductively coupled plasma atomic emission spectrometry (ICP-AES), and inductively coupled plasma mass spectrometry (ICP-MS).

SEM analysis was performed at the Qingdao Institute of Marine Geology under the following conditions: secondary electron resolution, 1.0 nm (15 kV) and 2.0 nm (1 kV); backscatter electronic resolution, 3.0 nm (15 kV); electron gun, cold field electronic source; accelerating voltage range, 0.5–30 kV (0.1 kV/step, variable); and magnification factor, ×(30–3 000).

Electronic probe analysis was conducted at the China University of Petroleum (East China), and microscopic texture and spectrum analysis were performed at the Shandong Key Laboratory for Oil and Gas Exploration, Shandong University of Science and Technology. A JXA-8230 super electronic probe microanalyzer (EPMA) (JEOL, Tokyo, Japan) was operated under the following conditions: secondary electron resolution, 6 nm; backscatter electronic resolution, 20 nm; spectrum channel number, 3CH; analytic element range, 5B–92U; accelerating voltage range, 0–30 kV; probe current range, 10^{-12}–10^{-5} A; and beam stability, $\pm 0.5\times10^{-3}$/h. Before measurement, samples were placed in a thermostat-controlled oven at 60°C for 1–2 h for dewatering, and were then glued to a 50 mm×50 mm platform with a conductive adhesive with the fresh sample section up. The dusts on sample surfaces was removed with a rubber pipette bulb, and the samples were then dried with an electric blower and numbered. Finally, specimens were sprayed twice with the vacuum coating equipment to create a uniform gold film with a thickness of 20 nm, and computer analysis was performed. For light elements with atomic numbers (Z)<32, the K series in Kα twin peaks or in the Kβ peak were generally used for calculation. For moderately heavy elements with

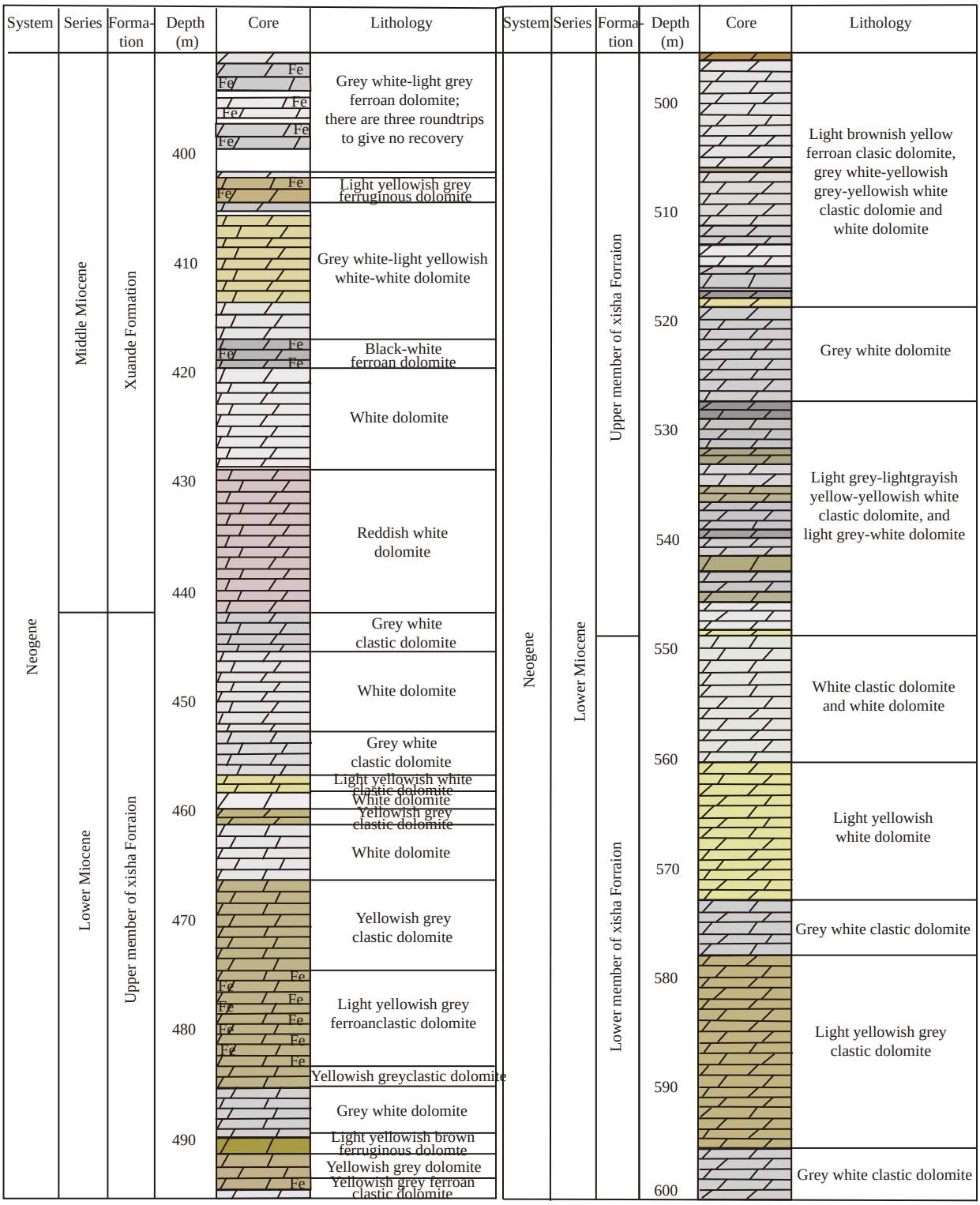

Fig.2 Columnar profile of Miocene sediments (390.04–600.33 m) in well Xiyong-2

$32 \leq Z \leq 72$, several L peaks were added; most had an α twin peak, followed by β and γ groups with higher energy, and the L series were used for calculation. For heavy elements with $Z > 72$, the M series was used for calculation because of the lack of K peaks and presence of M and L peaks.

ICP-AES and ICP-MS were employed to analyze the chemical compositions of whole rocks at the Qingdao Institute of Marine Geology. An agate mortar was used to mill 20 g of each sample to grain sizes of

less than 180 mesh. Then, samples were dried for 5 h at 110°C, and ca. 0.10 g of each dried powder sample was added to 15 mL of perfluoroalkoxy (PFA) in a vial. Each vial was sealed after 3 mL of HF and 2 mL of HNO_3 were added to the solution, placed on an electric heating board and kept at 185°C for 48 h. After a given vial was removed from the board and cooled, 0.5 mL of $HClO_4$ was added; the vial was again placed on the heating board and heated at 200°C for evaporation until the white smoke disappeared. Next, 5 mL of 1:1 HNO_3 was added to the vial, and the vial was sealed. The salts were allowed to re-dissolve for 12 h at 120°C. After cooling, the solution was moved to a 100-mL volumetric flask with deionized water and shaken before use. An IRIS Istrepid II XSP full-spectrum direct-reading plasma spectrometer (Thermo Scientific, MA, USA) was used to measure the concentrations of major elements (Fe, Al, Ca, Mg, K, Na, Mn, P, Ba, Sr, Zn, and Cu), and an XSERIES2 inductively coupled plasma mass spectrometer (ICP-MS) (Thermo Scientific, MA, USA) was used to detect the contents of minor elements (Li, Sc, Cr, Ni, U, Th, Rb, Co, Mo, Cs, W, Tl, and Y). The contents of calcium/magnesium carbonates were measured using 8% acetic acid and ICP-AES. HF was used to dissolve samples in sealed vessel, and their SiO_2 contents were measured using ICP-AES. The gravimetric method was used to evaluate loss on ignition.

A total of 17 samples were analyzed with XRD at the Qingdao Institute of Marine Geology using a D/MAX-2500 X-ray diffractometer (Rigaku, Japan) under the conditions of 40 kV, 100 mA, 10–70 (scanned area), 0.02 (step length), and 0.2 s (integral time).

3 RESULT

3.1 Core catalog results from drilling sections

3.1.1 Vertical distribution and characteristics of yellowish brown carbonate sediments along the drilling profile

As shown in Fig.2, round trip 1 (390.04–391.90 m) of the core illustrates a normal bioherm succession with milky white and gray-white limestone. Round trip 2 (391.9 m and below) shows yellowish-brown sediments, which are likely pyroclastic in origin; these sediments are distributed in six depth intervals as follows (Fig.3):

Layer 1: 401.75–404.51 m from round trip 8 (Fig.2), contains a large number of dark gray-black quasi-pyroclasts mainly composed of about 7% Fe oxides.

Layer 2: 405.2–405.71 m from round trip 10. The lower member mainly consists of light yellow–gray white calcirudite with minor volcanic clasts; the upper member is composed of dark brown–rust-colored quasi-volcanic tuff, 25% of which is volcanic breccia.

Layer 3: 417.11–419.77 m from round trip 14, mainly dark brown quasi-volcanic breccia limestone; the core is moderately broken with pyroclastic content of about 15%.

Layer 4: 474.75–483.52 m from round trips 32–34, mainly gray-white, light yellow and grayish yellow quasi-volcanic arenite-rudite, ranging from 5% to 25% in content. In the interval of 479.9–480.22 m, the volcanic clast content rises abruptly to 50% or more. Below 480.22 m, the contents of volcanic breccias decreases to 8%; the bottom core surface is covered with mesh-like quasi-pyroclastic sediments, which compose about 15% of the material.

Layer 5: 490.10–491.5 m from round trip 38; over 90% is quasi-pyroclasts.

Layer 6: 493.6–496.6 m from round trip 39. At the depths of 493.63–494.4 m, the core consists of yellowish gray to yellowish brown calcirudite with quasi-pyroclasts, the contents of which increase abruptly to 30%–40%. At the depths of 494.4–495.1 m, the core becomes dark gray–reddish brown, soft and brittle volcanic breccia limestone, with 90% quasi-pyroclasts and a thickness of up to 51 cm. At the depths of 495.1–496.6 m, the pyroclasts decrease markedly to less than 5%.

Recently, the genesis of the six brown sediment layers has been a matter of discussion. Some investigators have suggested that they were volcaniclastic rocks as initially described, whereas others have proposed that they were carbonates.

3.1.2 Observation of hand specimens

Some of yellowish brown to black sediments from round trip 39 were selected as specimens for testing (the 3/3 pipe-like sample of interval from 494.3–494.7 m depth, hereafter referred to as sample No. 9).

The hand specimens are reddish brown, brownish yellow, iron brown, rusty, yellowish gray white, and/or black in color. Most are loose and light in weight, and resemble yellowish-gray to white carbonate rocks, dissimilar to the yellowish brown–black carbonate sediments from round trips 2–7 (Fig.2), which are patchy, and also differ in appearance from the Dongdao volcanic pumices.

3.2 Lithological features of carbonate sediments

Sample No. 9 was sliced into thin sections, which were stained with alizarin red, to determine the types of reef-building organisms (such as sea urchins) in the background bioherm rocks. The image observations revealed black and gray-white sediments, yellow cements, bio-remains, and mineral grains of dolomite and calcite. Under magnification, the yellow cements are somewhat vitreous, with microscopic features similar to those typical of the Dongdao volcanic pumice.

3.3 Microscopic features of carbonate sediments

We employed an S-4800 cold-field scanning electron microscope (Hitachi, Tokyo, Japan) to identify the different kinds of minerals with various textures observed in sample No. 9. The SEM images and measurements illustrate occurrences of minerals

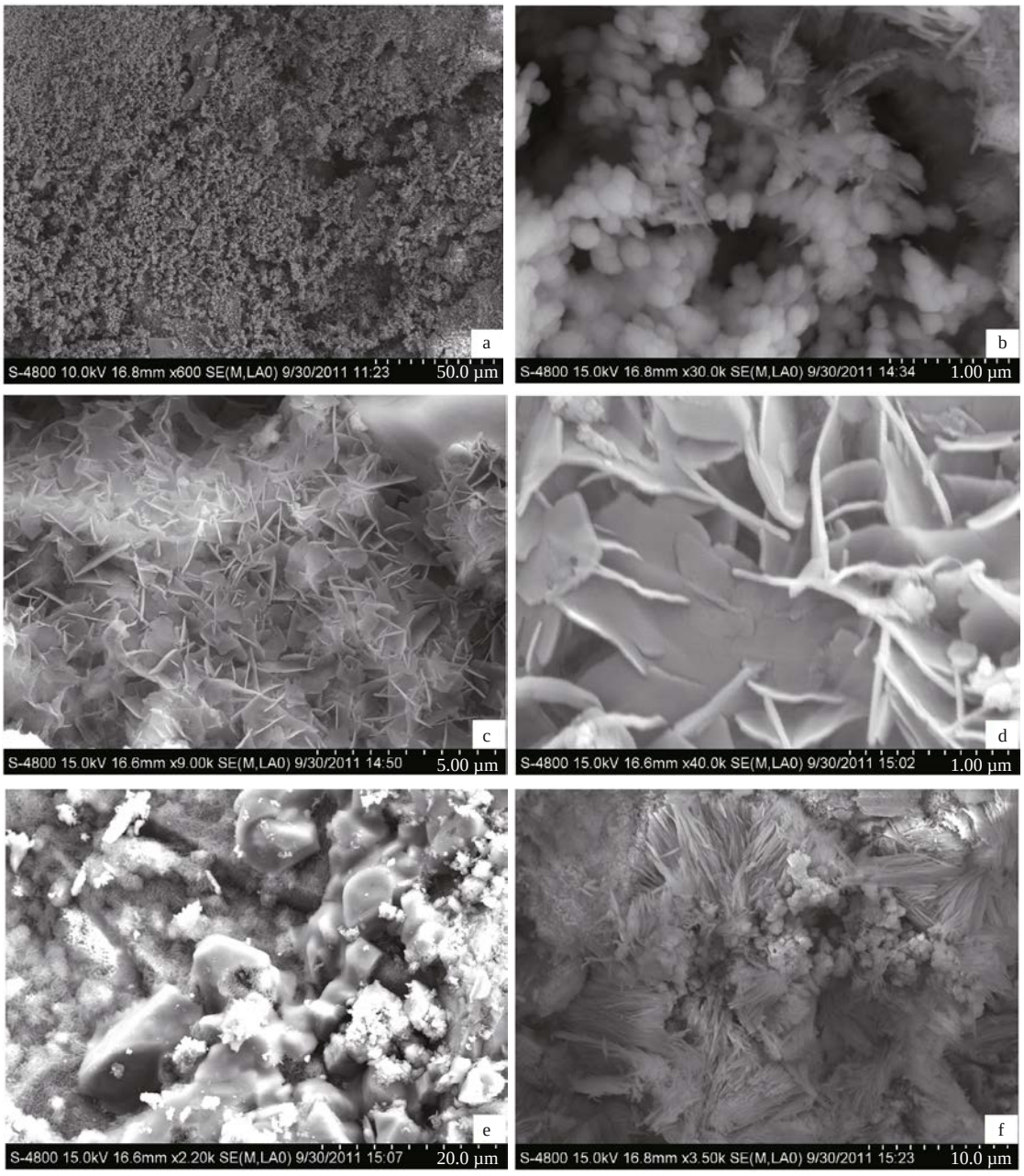

Fig.3 SEM images of different minerals and their assemblages in sample No. 9

a. clastic iron oxide; b. grape-like calcite; c. and d. scaly Ca-Mg oxide, i.e., periclase derived from dolomite at high temperatures; e. granular calcite; f. fibrous and granular iron oxide; g. fibrous iron oxide; h. scaly dolomite and granular iron oxide; i. columnar calcite; j. rhombohedral dolomite; k and l. flaky calcite; m. clastic iron oxide; n. granular calcite overlain by scaly calcite.

To be continued

Fig.3 Continued

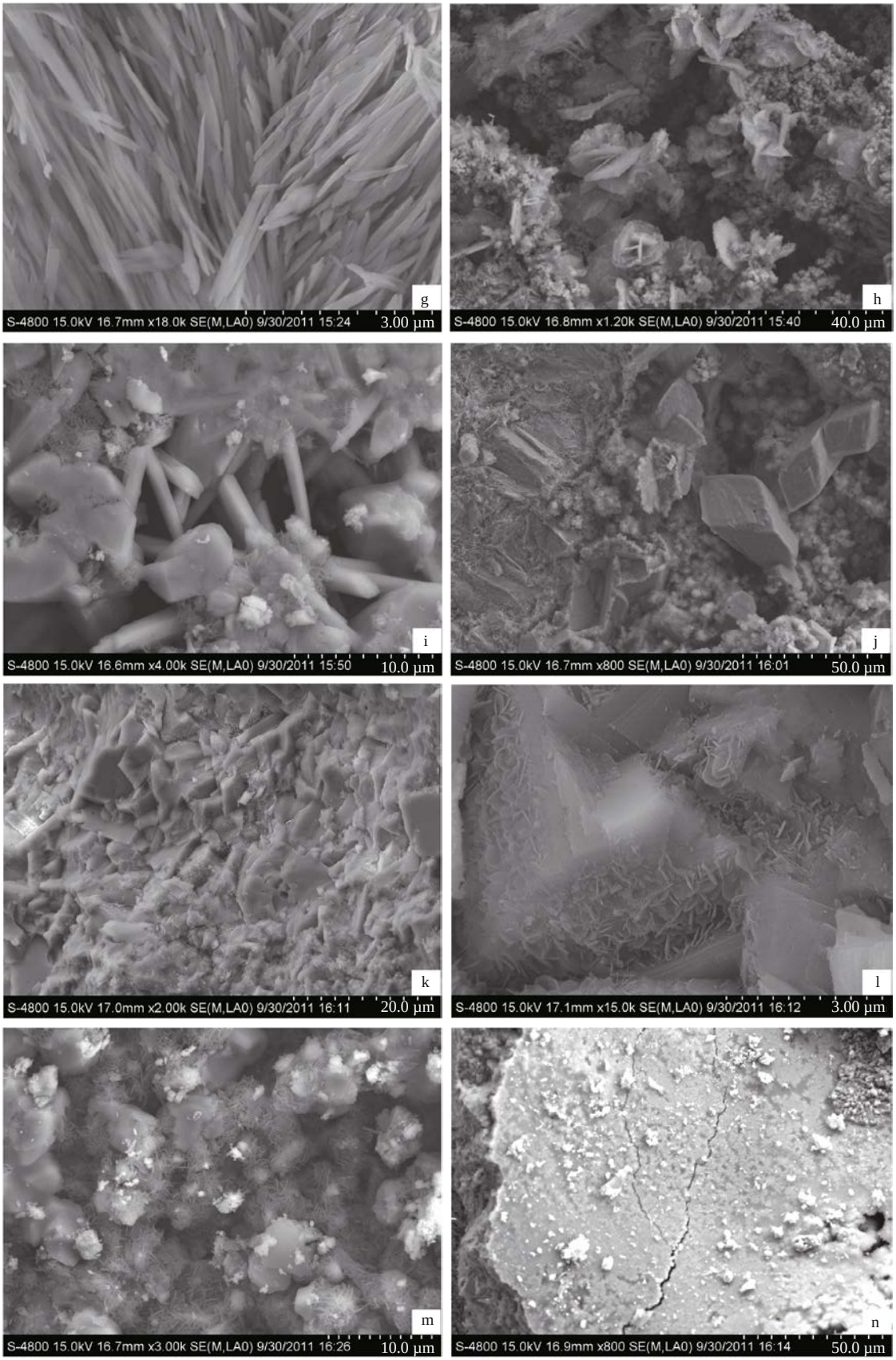

with multiple micro-textures, including fragmental (a, m), grape-shaped (b), scaly (c, d), granular (e), and fibrous (f, g) textures. In addition, various complex textures formed by two or more minerals were observed (h, i, j, k, l, m, n, n, and i), such as rhombohedral dolomite crystals, flaky minerals, columnar, striped, grape-like, and granular calcite crystals, and in particular the occurrence of iron oxides with different shapes (Fig.3).

Table 1 Chemical compositions of minerals in sample No. 9*

	A	B	C
Na_2O	0.084	0.067	0.088
SiO_2	0.197	1.114	0.266
Al_2O_3	-	-	0.012
MgO	0.200	0.231	0.071
F	-	-	-
CaO	0.280	0.281	0.176
BaO	-	-	0.015
P_2O_5	-	-	0.069
Cl	0.061	0.082	0.209
TiO_2	-	-	0.043
SO_3	0.083	0.020	0.054
K_2O	0.002	0.007	0.015
MnO	0.325	0.238	0.231
FeO	27.978	27.926	27.953
ZnO	-	-	0.126
Cr_2O_3	-	-	0.005
NiO	0.008	0.018	-
CuO	0.022	-	-
CoO	0.101	0.145	0.086
Total	29.327	30.110	29.372

3.4 Chemical compositions of minerals in ferroan dolomite rocks and detrital carbonate sediments

Sample No. 9 has typical bright and dark areas, as shown at the six measuring points A–F. The data of electron probe analysis are presented in Table 1. Component variations, bubbles and white smoke were observed when the dark areas were measured.

3.5 Chemical compositions of ferroan dolomite rocks and detrital carbonate sediments

The whole-rock chemical composition of sample No. 9 shows that the major elements included Ca, Fe, and Mg (Table 2; Fig.4). In addition, the contents of Cu, W, Zn, and Cr were high, whereas Sr was low. $CaCO_3$ and $MgCO_3$ were measured separately and yielded percentages of 40.78% and 26.73%, respectively. The SiO_2 content was only 0.60% (Table 3).

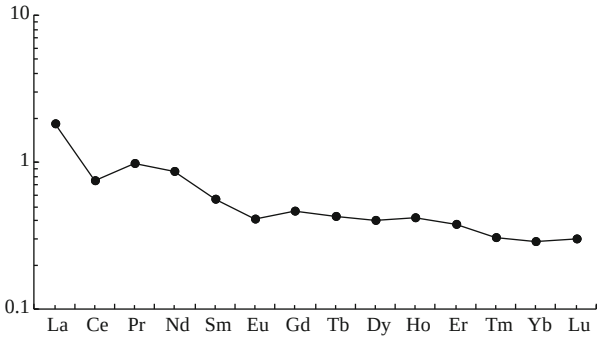

Fig.4 REE patterns of a ferroan dolomite

Table 2 Chemical composition of sample No. 9

ω(x)/10^{-2}						ω(x)/10^{-2}						
$CaCO_3$		$MgCO_3$		Ba		Co		Cu		Sr		Zn
40.78		26.73		5.15		75.5		940		197		353
ω(x)/10^{-6}												
Li	Sc	Cr	Th	Ni	Rb	Y	U	Mo	Cs	La	Ce	Pr
1.02	0.14	306.0	0.08	78.4	0.93	1.03	0.60	24.3	0.03	0.57	0.60	0.12
ω(x)/10^{-6}												
Nd	Sm	Eu	Gd	Tb	Dy	Ho	Er	Tm	Yb	Lu	W	Tl
0.52	0.11	0.03	0.12	0.02	0.13	0.03	0.08	0.01	0.06	0.01	583	0.02

Table 3 Contents of major elements (wt%) in sample No. 9*

CaO	MgO	Fe_2O_3	Al_2O_3	K_2O	MnO	Na_2O	P_2O_5	SiO_2	TiO_2	LOI	Total
22.83	12.73	29.76	0.12	0.025	0.28	0.19	0.03	0.60	0.004	34.19	100.76

* Fe_2O_3 is as TFe.

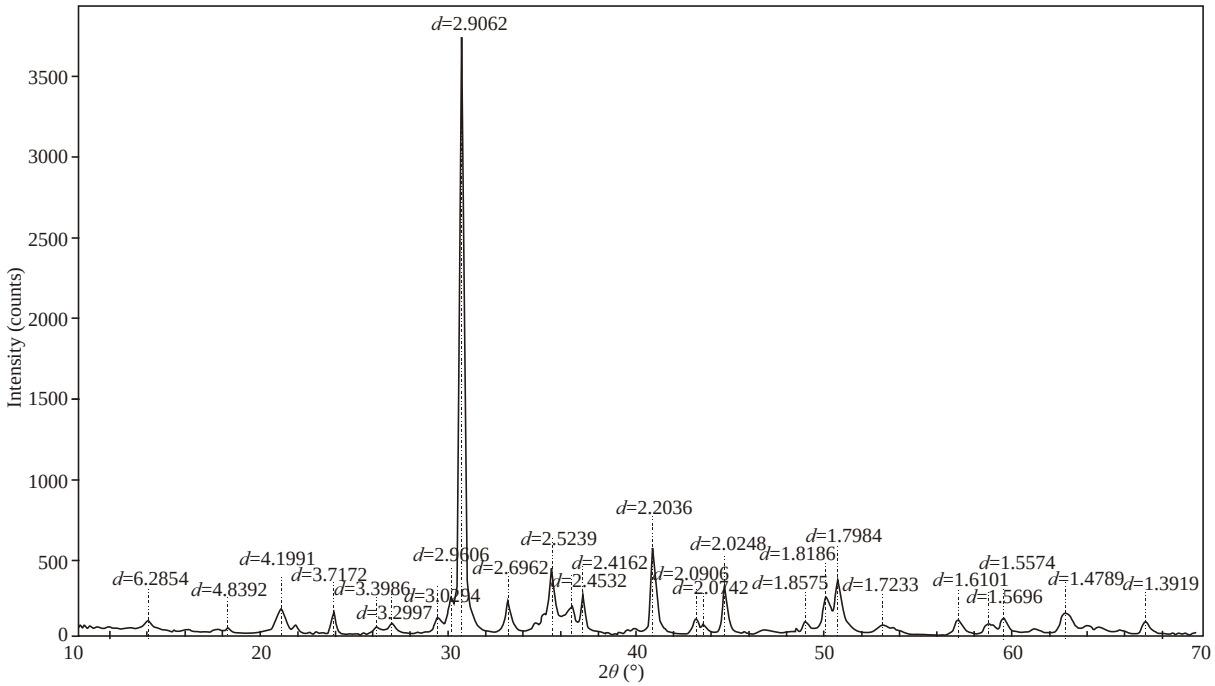

Fig.5 XRD spectrogram for sample No. 9 (*d*=2.906 2 for ankerite)

Table 4 Phase correlation in XRD spectrograms of core samples from well Xiyong-2

Nos.	Depth (m)	FOM* (matching ratio to ankerite)	FOM* (matching ratio to ankerite)	FOM* (matching ratio to ankerite)
1	392.5–393.5	3.4	26.9	0.7
2	405.1–405.5	5.4	5.4	0
3	417.5–418	4.5	12.4	1.8
4	436.3–436.5	2.1	6.4	0
5	439.5–440	2.0	8.1	0
6	477.15–480.22	2.0	6.1	0
7	483.2–483.5	2.6	5.5	0
8	487.35–487.5	2.2	7.4	0
9	489.3–489.7	4.9	10.7	0
10	490.5–490.8	1.9	8.5	0
11	493.5–493.7	5.0	8.6	0
12	494–494.3	4.1	10.3	0
13	495–495.3	6.1	18.1	0
14	507.7–507.8	2.7	12.3	0
15	540.36–540.6	2.8	17.0	0
16	553.8–554.0	6.0	20.6	0

* FOM is the matching ratio to a certain phase in the Jade interpretation software; smaller numbers indicate higher matching ratios, and zero indicates non-existence of this phase.

3.6 Mineral phases in ferroan dolostones and detrital carbonate sediments

The XRD identification indices indicated the presence of ankerite. Sample No. 9 was first measured using the XRD method (Fig.5). Compared with the 33-0282 card graph for ankerite (*d*=2.906 2) from the standard PDF card base, the spectrogram of sample No. 9 showed a perfect reflection peak of *d*=2.906 2, which is typical of ankerite and identical to that in the standard card graph (Yu et al., 2011). Furthermore, 16 core samples of different shapes and colors from different depths along the drilling core were analyzed using XRD (Figs.6 and 7), and the results from the Jade interpretation software show the matching ratios of 5.4–26.9 to dolomite, 1.9–6.1 to ankerite, and

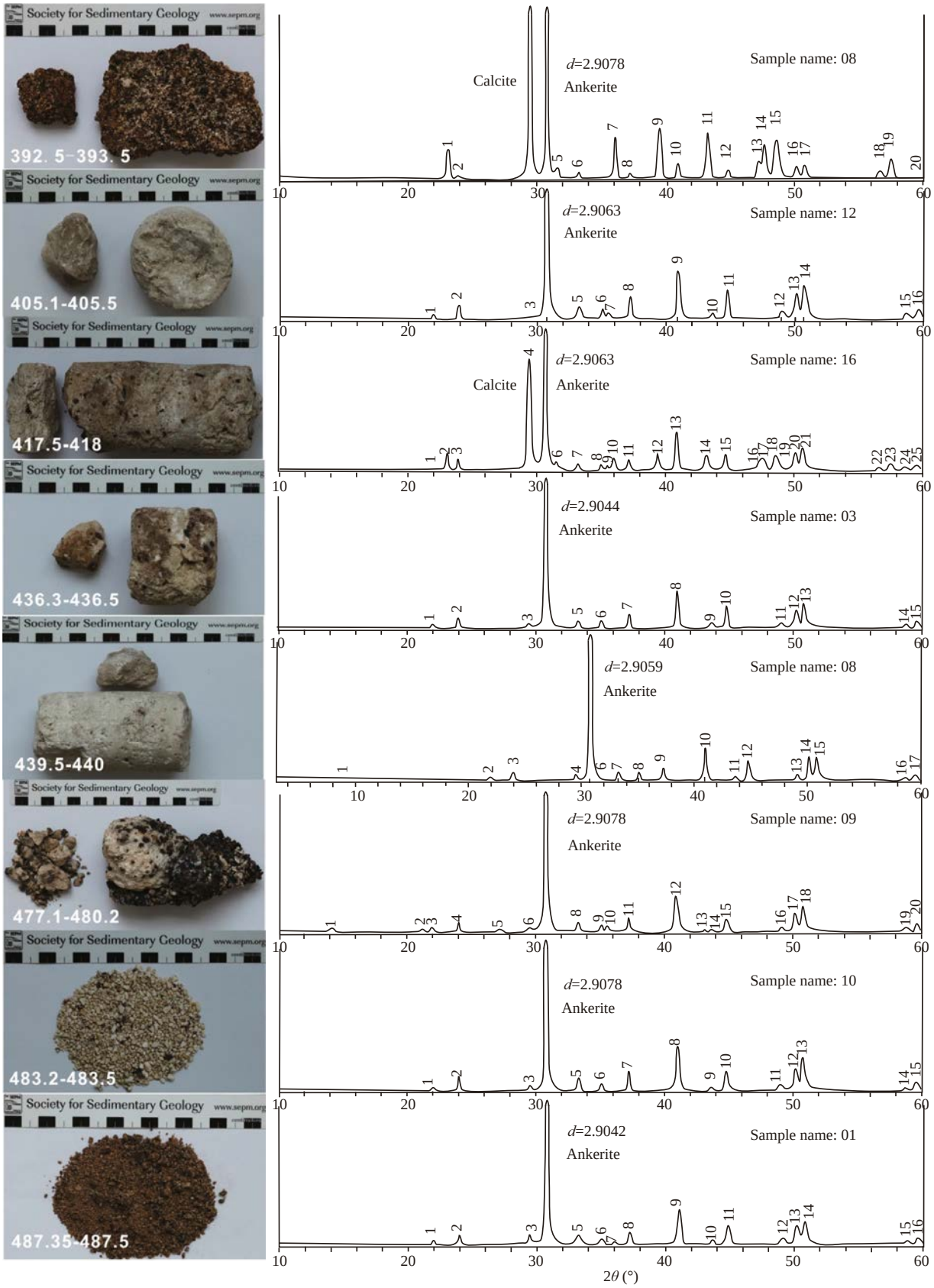

Fig.6 Photos and X-ray powder diffraction spectrograms of core samples from 392.5–487.5 m in well Xiyong-2

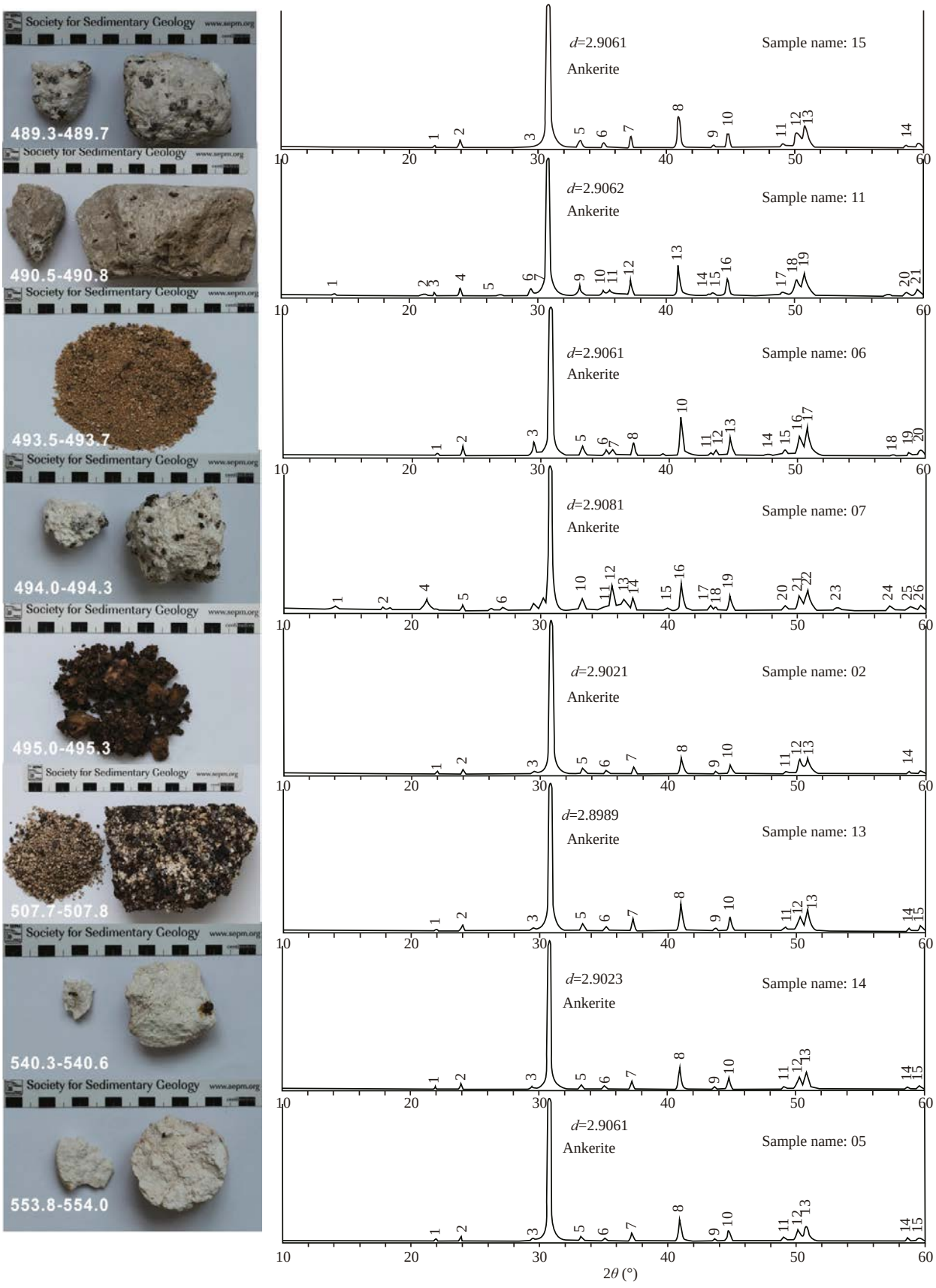

Fig.7 Photos and XRD spectrograms of core samples from 499.3 m to 554.0 m in well Xiyong-2

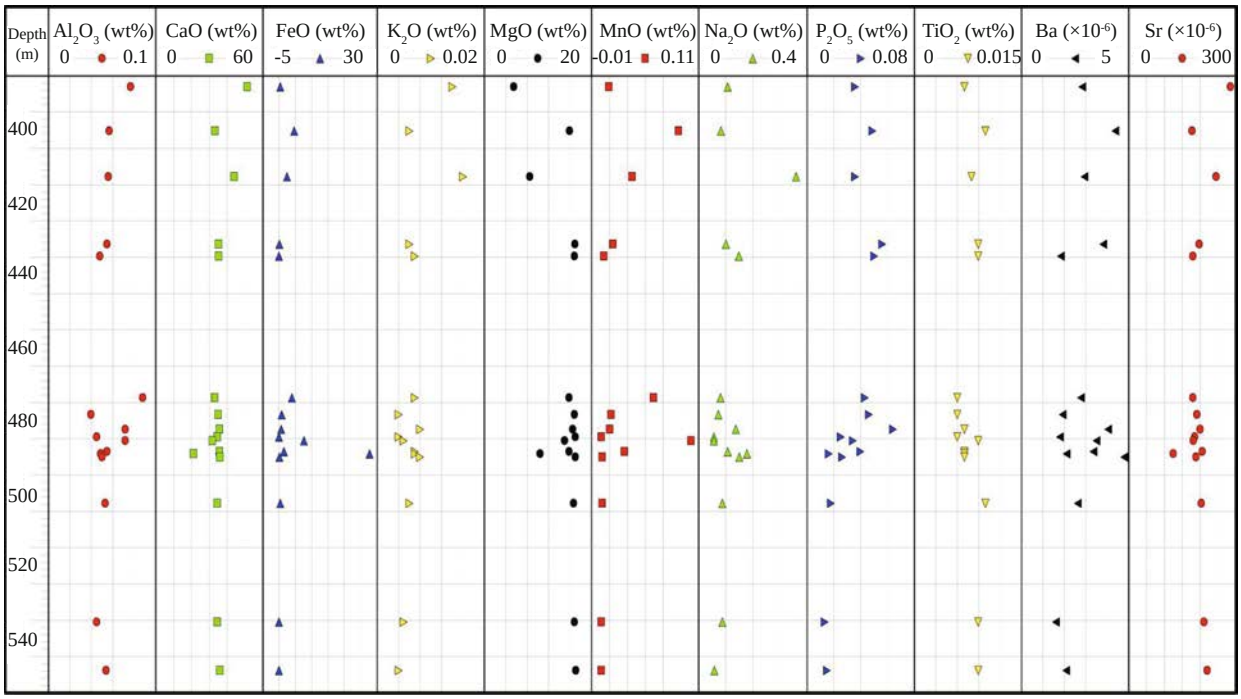

Fig.8 Contents of major elements in samples No. 1–16 from well Xiyong-2

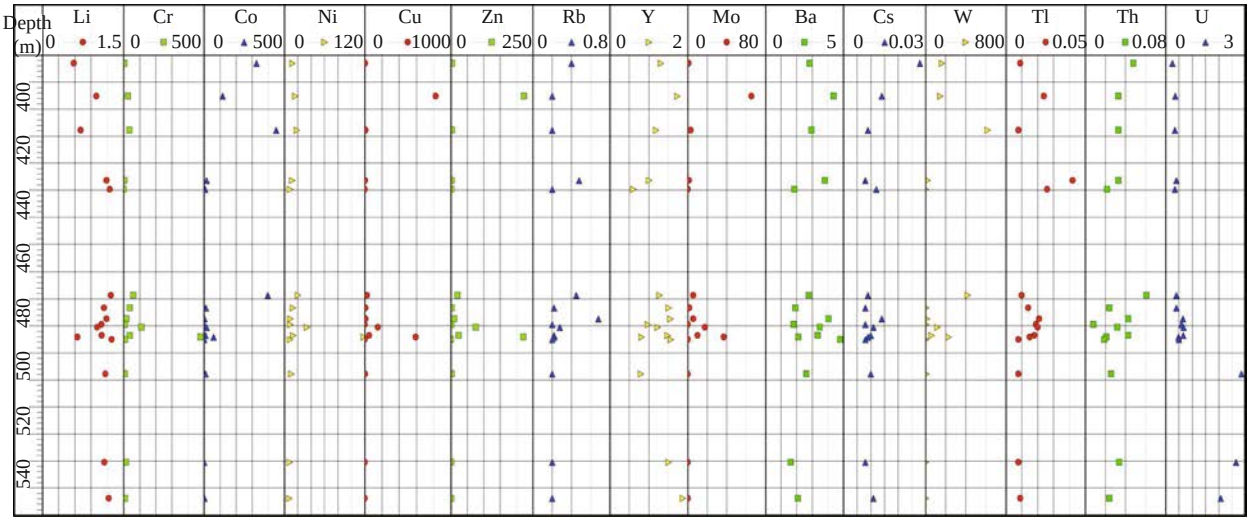

Fig.9 Contents of trace elements (10^{-6}) in core samples No. 1–16 from well Xiyong-2

mostly zero to calcite (Table 4). Measurements of metal elements indicated that the contents of Fe, Cu, W, Zn, Cr, Ni, Co, and Mo were very high (0.01%–27.78%; Fig.8), whereas the Sr content was low (Fig.9).

4 DISCUSSION

4.1 Compositions and types of ferroan dolomite rocks and detrital carbonate sediments

Ca, Fe, and Mg are three major elements in ferroan dolomite, but the most important characteristic is that it should have the composition of dolomite. As mentioned above, our core samples had a Ca/Mg ratio of 1.53, which is typical for dolomite (standard Ca/Mg ratios=1.5–1.7). The total Fe concentrations were high and varied greatly (0.014%–29.76%). Mn, Cu, W, Zn, Cr, Sr, and Ni had abnormally high contents. The yellowish brown ferroan dolomite and detrital carbonate sediments at depths of 392–554 m in well Xiyong-2 were characterized by low silica contents, and mainly consisted of rhombohedral ankerite, based on SEM and XRD analyses. According to the classification scheme illustrated in Fig.10, a rock with 25%–50% iron is classified as a ferroan carbonate.

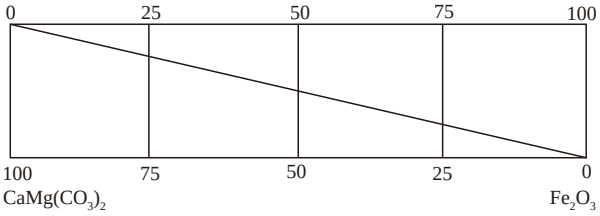

Fig.10 Classification diagram for ferroan dolomite

4.2 Sources and sedimentation mechanisms of Fe and other metals

Previous studies of the Xisha organic reefs (below a depth of 391 m) concluded that the reefs consist of white-gray, white-light grayish yellow normal bioherm sequences. However, this study shows that yellow-brownish black sediments, which are not of organic reefs, occurred at a depth of 391 m in well Xiyong-2.

The Xisha Islands are far from any continent, and lie in a continental-slope-type isolated carbonate platform environment (Wang, 2001). Therefore, the iron in the core samples could not have come from mainland China or from Hainan Island. The possibility of an iron source from a weathering unconformity in the periphery of the area is difficult to reconcile with the fact that the iron-rich sediments are not composed of silicates. Another possibility is a submarine hydrothermal source; however, no plate movement has been detected near the Xisha Islands. A source from volcanic eruptions is also unlikely because the samples do not contain pyroclastic sedimentary rocks. Thus, our analysis indicates that the core samples from well Xiyong-2 reflect paleoceanographic changes (Xu et al., 1999) in the South China Sea and in the sedimentary environment in the island-reef area of the study site.

The segment of well Xiyong-2 studied here is of Miocene age. Previous studies confirmed that a regional weathering unconformity developed during the Miocene (16 Ma) in the South China Sea. From an ODP 1148 core, a 14-m thick unconformity was found for the interval of 25.5–23.8 Ma, with a sedimentary hiatus of 1.5 Ma (Shao et al., 2004; Pang et al., 2007). However, this unconformity, which formed at the beginning of early Miocene, should lie below the recently discovered ferroan dolomite (Fig.2). Thus, it is beyond the range of the well segment of the present study, and only the unconformity at 16 Ma may be related to the recent discovery. Even if such an unconformity indeed existed in the isolated carbonate platform of the Xisha area, which formed in a low uplift process, it is difficult to explain the formation of over 100 m of thick, yellowish brown-black bioherm sediments. Calculated at a typical sedimentation rate, it would take millions of years to form an organic reef as thick as 100 m. Therefore, it is unlikely that Fe and other metals derived from these abnormal reefal sediments came from an unconformity. Furthermore, the same yellowish brown–black Fe-bearing succession was not observed from well Xichen-1 (on Chenhang Island of the Yongle Atoll), which is only about 100 km from Yongxing Island in the Xuande Atoll where well Xiyong-2 was drilled (Xu et al., 1999a). Therefore, the sediments rich in Fe and other metals were not related to the regionally developed unconformity.

The proposal that these sediments were related to submarine hydrothermal venting cannot be verified because no evidence has been found of the development or presence of submarine hydrothermal vents in the area.

If the metal elements were related to volcanic particles, they would likely be derived from Gaojianshi Island, 47 km southeast of Yongxing Island. This volcanic island is the sole material source of Fe and heavy metals in the region and would explain the lack of silicate rock in the core samples. During the middle Miocene, the volcanic activity on Gaojianshi Island was vigorous, and the lavas were fractionated in the air and sea during volcanic eruptions. In addition, volcanic ejecta, which included silicates, condensed, sank and was deposited in the Gaojianshi Island area after entering the seawater. Heavy metals, including but not limited to iron, were rapidly dissolved in seawater, and increased their solubility in seawater in the form of a colloidal solution, or sol. The prevailing winds pushed sea currents that carried such sol-like sediments to local reef areas of Yongxing Island. Multi-phase volcanic eruptions must have occurred, and resulted in a number of layers with the high Fe contents and high-temperature sediments (Wei et al., 2006).

The distance between the volcanic crater and the sedimentary area suggests that heavy metals (such as Fe) entrained by sols underwent long-distance transport. Accordingly, volcanic breccias did not occur in the core. Because of the joint effects of gravitational differentiation, intensive alteration, and oxidation, Fe and heavy metals such as Mn, Cu, W, Zn, Cr, Sr, and Ni would have dissolved from volcaniclastics. Consequently, Fe and heavy metals were enriched, whereas Si was depleted because of

the distance between the bioherm sedimentary area and the crater. Under the action of prevailing winds in the bi-directional monsoon area, in the South China Sea (Ye et al., 1984, 1985a; Zhang et al., 1987), winds enhanced the translocation of high-energy waves (Ye et al., 1985b), and created a sedimentation mechanism with two driving forces: sea currents and prevailing winds.

4.3 Genetic mechanism of dolomitization

The genetic mechanism of dolomitization has long been a topic of debate. Over ten different models have been proposed to interpret the genetic mechanism of dolomitization (Warren, 2000; Machel, 2004, 2005; Hu et al., 2011). However, all of these models are focused only on the genetic mechanism of pure dolomites based on foreign case studies. Up to date, pure dolomites formed in natural environments have not been found. Therefore, some investigators have questioned if naturally produced pure ankerite [$CaFe(CO_3)_2$] exists (Сыромятников and Воробьев, 1976). However, the iron dolomite and ferroan dolomite in this study were formed in a specific bioherm environment (Veizer, 1983) (Fig.10), an isolated carbonate platform on the continental slope far from land. It is clearly unique and different from previous findings that the massive iron occurred in a bioherm environment far from land. In fact, our newly-obtained XRD data indicate that the typical iron dolomite minerals were continuously distributed in the area around well Xiyong-2 across hundred meters in the late Miocene. Therefore, the environment of the Xisha Islands and the ancient South China Sea in the late Miocene underwent one significant change for a continuous supply of massive iron and other heavy metals from an unknown source for about one million years. How this immense amount of metals accumulated in the study area has remained a mystery. This process is related to the changes of the ancient South China Sea, and may remotely correspond to the Mediterranean salinity crisis of the same interval of time (He et al., 1982). This evidence also confirms the occurrence of events in the South China Sea (Xu et al., 1999). Importantly, our discovery not only confirms the existence of a late Miocene paleoceanographic event in the South China Sea, but also reminds us to focus on determining the source of massive metals in iron dolomites in the study area. As mentioned above, dolomitization in well Xichen-1 was related to the global glacial regression in the Miocene. In light of our new data, we suggest that the Miocene regression occurred at the depth of 135.51 m based on the Sr contents in this well, and that the mixing of seawater and fresh water may have induced the onset of dolomitization (He and Zhang, 1990; Xu et al., 1994, 1999b; Wei et al., 2007). In the processes described above, massive heavy metals from volcanic eruptions on Gaojianshi Island were entrained by sea currents for deposition in the Yongxing Island area. Finally, these sediments were dolomitized via an extensive Fe-Mg exchange, and ferroan dolomites were formed, as observed in well Xiyong-2 (Fig.11).

4.4 Significance of bioherm dolomites in the South China Sea

The largest oilfield in the South China Sea is the Liuhua 11-1 oilfield in the vast organic reef area of the Pearl River Mouth Basin, and the largest gas field lies in Organic Reef L of the Zengmu Basin. The reservoirs of the two fields belong to the bioherm dolomites formed in the Miocene (May and Eyles, 1985; Lü et al., 2002), which is consistent with the well intervals in the present study. Comparison of results from worldwide petroleum exploration suggests that many reservoirs are composed of dolomites. Zenger et al. (1980) showed that more than 50% of carbonate reservoirs worldwide (nearly 80% of North American reservoirs) formed in dolomites. Although these statistical data were published several decades ago, dolomites are still considered to be the most important global oil reservoirs because the discovery of carbonate hydrocarbon deposits peaked globally during the 1950s–1970s. In 1984, China had an important discovery of Paleozoic carbonate petroleum through well Shacan-2 in the Tarim Basin, and then in well Tashen-1 at a depth of 8 408 m in the same basin, where Paleozoic dolomites (Chen et al., 2008, 2010; Zhu et al., 2008) and microbiogenic dolomites of the Middle and Upper Cambrian Series (You et al., 2013) were discovered.

Large gas fields in the Puguang, Longgang, and Yuanba areas of Sichuan Province, China were also found in dolomite reservoirs (Huang et al., 2008). In the 1980s, large oil/gas fields were discovered in the South China Sea, and similar findings were reported several decades ago. Perhaps no relevant research is currently underway in China, or sufficient systematic core data to support petroleum drilling may be lacking. Moore (2008) reported that the lack of newly-developed dolomite evolution models is a factor that has restricted breakthroughs in petroleum exploration in marine carbonate rocks. Therefore, studies on

dolomites formed in the unique environments of island reef areas and investigations of their evolution are of great practical significance to supplement theoretical dolomite data and to elucidate the characteristics of Miocene petroleum reservoirs in the South China Sea Basin.

5 CONCLUSION

In the more than 100-m-thick organic reef profile at the depth interval of 390.04–600.33 m in well Xiyong-2, we discovered six sediment layers that appeared to be volcaniclastic sediments. These layers in the multicolored drilled core occurred as thin beds intercalated with white or light gray dolomite and were of late-middle Miocene age.

Petrological observations and systematic measurements collected using SEM, EDS, ICP-AES and ICP-MS and XRD indicate that the ferroan dolomite and carbonate detrital sediments have low Si contents but high concentrations of Fe, Mn, Cu, W, Zn, Cr, Ni, and Co; their Sr contents are lower than the accepted Sr boundary value for a normal dolomite.

Based on our newly obtained results, the formation of these ferroan dolomites may have proceeded roughly as follows: the high contents of Fe and other heavy metals were preferentially derived from sols produced by the volcanic activity on Gaojianshi Island. These metals were transported into the Yongxing Island area via two driving forces, prevailing winds and sea currents/tides. These metals ultimately were deposited and formed a unique organic reef profile with the multiple layers of sediments rich in Fe and other heavy metals. In the late Miocene, the isolated Xisha carbonate platform was subaerially exposed and experienced a freshwater leaching, which resulted in dolomitization induced by mixing between sea water and fresh water. One extensive Fe-Mg exchange may have lasted for a prolonged period of time during the formation of organic reefs with ferroan dolomites.

6 ACKNOWLEDGMENT

The authors express their sincere thanks to CAS Academicians JIN Qinghuan and QIN Yunshan and Prof. LI Sitian for their long-term support and help, and to Prof. HE Qixiang for encouraging us to write this paper.

References

Сыромятников, Воробьев. 1976. Experiments of Ankerite Replacing Calcite. Translation Chen G X, trans. Geology-Geochemistry. p.22-25.

Chen Y Q, Zhou X Y, Yang H J. 2010. Geochemical research and genesis of dolostones with different crystal characteristics occurring in the Upper Cambrian, centeral area of Tarim Basin. *Acta Sedimentologica Sinica*, **28**(2): 209-218. (in Chinese with English abstract)

Chen Y Q, Zhou X Y, Zhao K D, Yang W J, Dong C Y, Zhu C J. 2008. Geochemical research on straticulate dolostone and spatulate dolostone in Lower Ordovician strata of well Tazhong-1, Tarim Basin. *Acta Geologica Sinica*, **82**(6): 826-834. (in Chinese with English abstract)

Han C R, Meng X Y. 1990. Foraminiferal fauna distribution in reef-facies beds since Late Miocene in Xisha Islands and its significance. *Marine Geology & Quaternary Geology*, **10**(2): 65-80. (in Chinese with English abstract)

He Q X, Zhang M S. 1986. Reef Geology of the Xisha Islands China. Science Press, Beijing, China. p.1-182.

He Q X, Zhang M S. 1990. Origin of Neogene dolomites in Xisha Islands and their significance. *Marine Geology & Quaternary Geology*, **10**(2): 45-55. (in Chinese with English abstract)

Hu Z W, Huang S J, Zhang C, Lang X G, Zhou H. 2011. A review of dolomitization models of carbonates. *Marine Geology Frontiers*, **27**(10): 1-13. (in Chinese with English abstract)

Huang S J, Qing H R, Hu Z W, Pei C R, Wang Q D, Wang C M, Gao X Y. 2008. Cathodoluminescence and diagenesis of the carbonate rocks in Feixianguan Formation of Triassic, eastern Sichuan Basin of China. *Earth Science—Journal of China University of Geosciences*, **33**(1): 26-34. (in Chinese with English abstract)

Lü B Q, Wang G Z, Quan S Q, Zhao X T. 1986. A preliminary study of the formation of Shidao Island, Xisha Islands. *Chinese Journal of Geology*, (1): 82-89. (in Chinese with English abstract)

Lü B Q, Wang G Z, Quan S Q. 1987. Sedimentary characteristics and evolutionary pattern of the sand cays in the Xisha Islands. *Marine Geology & Quaternary Geology*, **7**(2): 59-69. (in Chinese with English abstract)

Lü B Q, Xu G Q, Wang H G, Zhao H M. 2002. Sea floor spreading recorded by drowning events of Cenozoic carbonate platforms in the South China Sea. *Chinese Journal of Geology*, **37**(4): 405-414. (in Chinese with English abstract)

Machel H G. 2004. Concepts and models of dolomitization: a critical reappraisal. *In*: Braithwaite C J R, Rizzi G, Darke G eds. The Geometry and Petrogenesis of Dolomite Hydrocarbon Reservoirs. Geological Society of London Special Publication, London. 235. p.7-63.

Machel H G. 2005. Investigations of burial diagenesis in carbonate hydrocarbon reservoir rocks. *Geoscience Canada*, **32**(3): 103-128.

May J A, Eyles D R. 1985. Well log and seismic character of tertiary terumbu carbonate, South China Sea, Indonesia. *AAPG Bulletin*, **69**(9): 1 339-1 358.

Meng X Y. 1989. Biostratigraphical boundaries and

environmental changes of Xisha Islands since late Miocene shown by foraminiferal fauna. *Acta Micropalaeontologica Sinica*, **6**(4): 345-356. (in Chinese with English abstract)

Moore C H. 2008. Carbonate Reservoirs: Diagenesis and Porosity Evolution in Sequence Stratigraphic Framework. Yao G S, Shen A J, Pan W Q, Zheng J F, Luo X Y, Han J F, trans. Petroleum Industry Press, Beijing.

Pang X, Chen C M, Peng D J, Zhou D, Chen H H. 2007. The Pearl River Deep-water Fan Systems & Petroleum in South China Sea. Science Press, Beijing. p.1-360.

Shao L, Li X H, Wang P X, Jian Z M, Wei G J, Pang X, Liu Y. 2004. Sedimentary record of the tectonic evolution of the South China Sea since the Oligocene—evidence from deep sea sediments of ODP site 1148. *Advances in Earth Science*, **19**(4): 539-544. (in Chinese with English abstract)

Veizer J. 1983. Trace elements and isotopes in sedimentary carbonates. *Reviews in Mineralogy and Geochemistry*, **11**(1): 265-299.

Wang G Z, Lü B Q, Quan S Q. 1986. The sedimentary environments and characteristics of the coral reef of the Yongxing Island. *Oceanologia et Limnologia Sinica*, **17**(1): 36-44. (in Chinese with English abstract)

Wang G Z. 2001. Sedimentology in Coral Reef Areas of the South China Sea. China Ocean Press, Beijing. p.1-313. (in Chinese)

Warren J. 2000. Dolomite: occurrence, evolution and economically important associations. Earth-Science Reviews, **52**(1-3): 1-81.

Wei X, Jia C Z, Meng W G, Xiong X H. 2008. Biogenetic reefs and its petrological characteristics of well Xichen 1, Xisha Sea Area, China. *Geological Bulletin of China*, **27**(11): 1 933-1 938. (in Chinese with English abstract)

Wei X, Jia C Z, Meng W G, Zhang F L. 2007. Mineral content and geochemistry characteristics of carbonate rock in well No. Xichen-1 and geological significance. *Acta Petrologica Sinica*, **23**(11): 3 015-3 025. (in Chinese with English abstract)

Wei X, Zhu Y J, Xu H, Zhao G C, Li Y X. 2006. Discussion on Neogene dolostone forming condition in Xisha Islands: evidences from isotope C and O and fluid inclosures. *Acta Petrologica Sinica*, **22**(9): 2 394-2 404. (in Chinese with English abstract)

Xu H, Cai F, Wang Y J, Gong J M, Gou Y X, Sun P, Zhang B G, Zhou L Y. 1999b. Evolution of Miocene organic reefs and functions of algae's reef-making in Xisha Islands. *Chinese Science Bulletin*, **44**(21): 1 996-2 001.

Xu H, Wang Y J, Cai F. 1999a. Miocene Biostratigraphy in the Xisha Islands: Reef-building by Algae and Bioherm Evolution. Science Press, Beijing. 164p. (in Chinese)

Xu H, Zhang J C, Cai F. 1994. Study and significance of miocene biohermal mineral facies in the Xisha Islands. *Marine Geology & Quaternary Geology*, **14**(4): 15-23. (in Chinese with English abstract)

Yan W, Tang X Z, Chen Z, Chen M H, Gu S C. 2002. The genesis and environmental significance of red and black sedimentary interlayers in coral reef of well Nanyong 2. *Chinese Science Bulletin*, **47**(4): 343-347.

Ye Z Z, He Q X, Zhang M S, Han C R, Li H, Ju L J, Wu J Z. 1985b. Type classification and characteristics of islands in the Xisha Archipelago. *Marine Geology & Quaternary Geology*, **5**(1): 1-13. (in Chinese with English abstract)

Ye Z Z, He Q X, Zhang M S, Han C R, Li H, Wu J Z, Ju L J. 1985a. The sedimentary structures and the facies model of the late Pleistocene Eolian biocalcarenites in Shidao Island of Xisha Archipelago. *Acta Sedimentologica Sinica*, **3**(1): 1-15. (in Chinese with English abstract)

Ye Z Z, Zhang M S, Han C R, Wu J Z, Li H, Ju L J. 1984. A new discovery on Shidao Island of Xisha Archipelago: eolianite (Eolian Calcarenite) and fossil soils. *Marine Geology & Quaternary Geology*, **4**(1): 1-10. (in Chinese with English abstract)

You X L, Sun S, Zhu J Q, Li Q, Hu W X, Dong H L. 2013. Microbially mediated dolomite in Cambrian stromatolites from the Tarim Basin, north-west China: implications for the role of organic substrate on dolomite precipitation. *Terra Nova*, **25**(5): 387-395, https://doi.org/10.1111/ter.12048.

Yu J S, Lei X R, Zhang J H, Wu H D. 2011. Mineral Identification Using X-ray Powder Diffraction Method. Huazhong University of Science and Technology Press, Wuhan. p.1-370. (in Chinese)

Zenger D H, Dunham J B, Ethington R L. 1980. Concepts and models of dolomitization. SEPM Special Publication No. 28, SEPM, Tulsa, OK, USA. p.1-328.

Zhan W H, Yao Y T, Zhang Z Q, Sun Z X, Zhan M Z, Sun L T, Liu Z F. 2006. Crustal activities recorded incoral reefs in the northwestern South China Sea. *Chinese Science Bulletin*, **51**(S2): 89-94.

Zhang M S, He Q X, Ye Z Z, Han C R, Li H, Wu J Z, Ju L J. 1987. Wind-driven model of reef facies: a new working hypothesis. *Marine Geology & Quaternary Geology*, **7**(2): 1-9. (in Chinese with English abstract)

Zhang M S, He Q X, Ye Z Z, Han C R, Li H, Wu J Z, Ju L J. 1989. Sedimentary Geology of Bioherm Carbonate in the Xisha Islands. Science Press, Beijing. p.15-68. (in Chinese)

Zhu J Q, Wu S Q, Wang G X, Hu W X. 2008. Types and porosity characteristics of the Cambrian-Ordovician Dolostones in Tarim basin. *Earth Science Frontiers*, **15**(2): 67-79. (in Chinese with English abstract)